Iran. J. Radiat. Res., 2011; 9(2): 109-119

Fabrication of low cost in-house slab homogeneous and heterogeneous phantoms for lung radiation treatment

S. Senthilkumar[1*] and V. Ramakrishnan[2]

[1]Department of Radiotherapy, Govt. Rajaji Hospital and Madurai Medical College, Maduari-625 020, India

[2]Deptartment of Laser Studies, Madurai Kamaraj University, Madurai, Tamil Nadu, India

Background: The heterogeneous composition of the human body presents numerous tissue types and cavities with widely differing radiologic properties. The aim of the present work was to develop a low cost homogeneous and heterogeneous phantom and the absorbed dose were measured by ionization chamber for different radiotherapy treatment techniques and compared with treatment planning system absorbed dose values. ***Materials and Methods:*** Present work deals with the fabrication of inexpensive homogeneous and heterogeneous tissue equivalent slab phantom using polymethyl methacrylate, cork, teflon and perspex as a tissue, lung, spine and tumor simulating materials respectively. These phantoms were used for different treatment techniques and full rotation techniques in SSD and SAD techniques. ***Results:*** The measured dose values for the different positions of both phantoms were compared with the TPS values. The values are coinciding with each other and the percentage of deviation varies from 0.47 to 2.8 and 0.49 to 2.86 for heterogeneous and homogeneous phantoms respectively. ***Conclusion:*** The measured values from ion chamber were compared with 3-D Plato Treatment Planning System (TPS). TPS values were also revealed the same result for homogeneous and heterogeneous phantoms. The dose value of tumor is found to be gradually decreased with increase in arc angle. The dose value of spine is also found to be gradually decreased up to 90° and increased in 360°. Heterogeneity correction would definitely improve the cancer treatment of the heterogeneity region. This in-house phantom is inexpensive, easy to handle and very useful one to verify the TPS calculation. **Iran. J. Radiat. Res., 2011; 9 (2): 109-119**

Keywords: *Homogeneous phantom, heterogeneous phantom, cork, teflon, perspex.*

INTRODUCTION

A primary objective in modern radiotherapy is to maximize the therapeutic benefit of radiation treatments which critically depends on delivering the prescribed dose to the target volume with high spatial precision and minimize the dose to the neighboring healthy tissues. Achieving this goal requires accurate spatial localization of all relevant structures and accurate calculation of the absorbed dose [(1)]. There are still some difficulties, such as the radiation beam geometric and dosimetric characterization of radiation fields [(2)]. Heterogeneity corrections in dose calculations are necessary for radiation therapy treatment plans [(3)]. The effect of heterogeneities on dose distributions and dose calculations is an issue that has concerned the medical physics community for almost three decades. Most studies have investigated low-density materials, more or less equivalent to lung [(4 -17)].

The human body consists of numerous tissue types and cavities like lungs, bones, teeth, sinuses, nasal and oral cavities with widely differing radiologic properties. Optimization of radiotherapeutic impact requires correct accounting for this heterogeneity so that absorbed dose may be accurately determined in all irradiated tissues [(18)]. The effects of air cavities on radiosurgical beams, shows a dose drop across the cavity. Subsequent buildup and dose enhancement on the distal side of the cavity have also been reported [(19-21)]. Accurately determining the dose in the regions of complex tissue heterogeneities, such as in

Corresponding author:
Dr. S. Senthilkumar,
Department of Radiotherapy, Govt. Rajaji Hospital and Madurai Medical College, Maduari-625 020, India.
E-mail: *sasenthilgh@gmail.com*

the thorax, is a current challenge in clinical trials for the reporting of consistent tumor and lung doses [22]. The accuracy of dose calculations using heterogeneity corrections have been evaluated mostly in studies of dose delivered along the central axis and in the penumbral regions based on simple beam geometries using slab phantoms [23, 24]. Other studies have compared the accuracy of treatment planning systems to Monte Carlo calculations from patient CT data sets [25-27]. Only limited data have been obtained for advanced systems designing treatment plans using anthropomorphic phantoms [28-30]. Simple homogeneous and heterogeneous spherical and cylindrical phantoms have also been used with ion chambers to monitor the delivered doses for multi-field plans [31, 32].

The aim of the present study was to develop a low cost homogeneous and heterogeneous phantom using polymethyl methacrylate (PMMA), cork, teflon and perspex for soft tissue, lung, spine and tumor substitutes respectively. These materials were selected for availability and low price and good machining property. Many holes were made in these phantoms in different areas to insert the cylindrical 0.6 cc ion chamber and measure the point doses. Measurements were done for different conventional lung treatment techniques for different field sizes, arc technique for different angles and also for full rotation techniques. Finally, these measured values were compared with 3D Plato TPS values.

MATERIALS AND METHODS

Heterogeneous phantom

PMMA, cork, teflon and perspex materials were used to fabricate the heterogeneous phantoms. PMMA is an amorphous thermoplastic which is optically transparent, unaffected by moisture and offers a high strength to weight ratio. PMMA and cork slabs dimensions were 30×30 cm^2 and with various thickness. Cylindrical shape teflon with 30 cm in length and 2.5 cm in diameter was used as stimulating material for spine. 30 cm length of perspex with 4×4 cm^2 cross section was used for tumor stimulating material.

The relative electron density of PMMA, cork, teflon and perspex was 1.02, 0.2, 2 and 1.18 g/cm^3 respectively in comparison with water. A hole (1.5 cm dia and 15 cm depth) was drilled exactly on the centre of teflon cylindrical rod and perspex square rod to insert the 0.6 cc ionization chamber. PMMA and cork are used as a stimulating material for soft tissue and lung respectively.

Homogeneous phantom

Homogeneous phantom was fabricated using 30 × 30 cm^2 dimensions of PMMA slab with various thicknesses (0.1 to 3 cm). A hole was drilled in one of the thickest (3 cm) slab to fit the ionization chamber.

Dose measurements

Figure1 shows the experimental setup of PMMA and cork slab phantom and the ion chamber inserted in the cork slab to measure the lung dose. The radiation measurements have been made from a cobalt-60 machine with a source to surface distance of 80 cm. The cobalt machine is Theratron Phoenix with average photon energy of 1.25 MeV. The dose measurements were performed using a CD-high tech secondary standard dosimeter SSD-92/090 cylindrical ionization chamber with 0.6 cm^3 volume, 5.5 mm diameter and 25.5 cm length, connected to a CD-high tech electrometer and calibrated at the Bhabha Atomic Research Center (BARC) secondary standard calibration laboratory. Due to its relatively large volume, Serago *et al.* [33] and Rustgi and Frye [34] recommended that this chamber could be used for field diameters greater than 20 mm. Therefore this chamber was used only for the largest field size measurements. Measurements were done for different treatment techniques for the field sizes vary from 5×5 to 35×35 cm^2. The experimental heterogeneity correction factor for each point was taken as the ratio

of readings with and without the presence of the inhomogeneity with the same geometric conditions.

Figure 1. Experimental setup of PMMA and cork slab phantom and the ion chamber inserted in the cork slab to measure the lung dose

Treatment techniques

Technique 1

In this technique, the heterogeneous phantom consists of two layers such as cork (9.8 cm thickness) and PMMA (5 cm thickness) and the homogeneous phantom consists of PMMA slabs with total thickness of 14.8 cm. Output measurements have been done using Co-60 machine for different field sizes varying from 5×5 to 35×35 cm^2, with a source to surface distance (SSD) of 80 cm.

The chamber was kept at 10 cm depth in both phantoms. The experimental set up for SSD technique is shown in figure 2. The same procedure was adopted for source to axis distance (SAD) technique in which chamber to source distance is 80 cm and the total thicknesses of the homogeneous and heterogeneous phantoms are same.

Technique 2

Figure 3 shows the experimental set up of homogeneous and heterogeneous phantoms. The cork with the thickness of 9.8 cm is placed between two PMMA slabs (5 cm thickness) to form a heterogeneous phantom. Homogeneous phantom with 19.8 cm thickness was used in the SSD and SAD techniques. The dose values were measured for various field sizes (5×5 to 35×35 cm^2) at the depth of 15 cm.

Technique 3

The heterogeneous phantom was built using PMMA and cork slabs in two ways: (i) three layers of PMMA (each 4 cm) and two layers of cork (each 4 cm) were alternatively placed one by one; (ii) 4 cm thickness of cork slab was placed between 12 and 4 cm thickness of PMMA slabs. Chamber was placed at a depth of 16.2 cm for both phantoms in SSD and SAD techniques (figure 4), various field sizes (5×5 to 35×35 cm^2) at the depth of 15 cm.

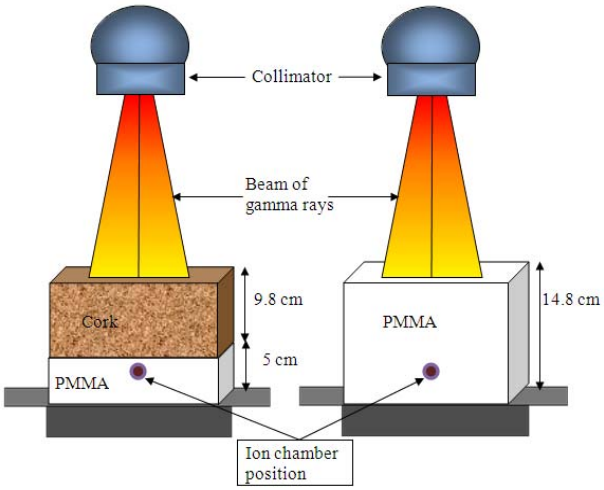

Figure 2. Experimental setup of (a) heterogeneous (cork+PMMA) and (b) homogeneous (PMMA) phantoms in SSD technique

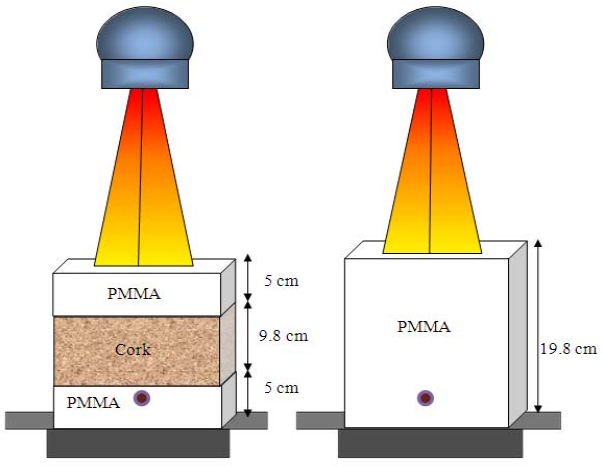

Figure 3. Experimental setup of (a) heterogeneous (PMMA+cork+ PMMA) and (b) homogeneous (PMMA) phantoms in SSD technique

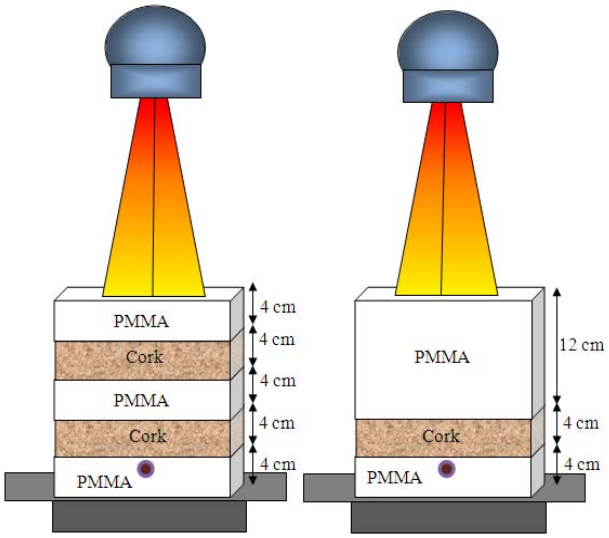

Figure 4. Experimental set up of different layers of hetero geneous phantoms.

Technique 4

Thoracic phantom consists of 7 and 4 cm thickness of PMMA slabs, 8 cm thickness of cork slab, 3 cm diameter of Teflon cylinder rod and 4 × 4 cm^2 square perspex block. The cork slab was placed between the PMMA slabs and teflon rod placed within the 4 cm thickness of PMMA slab. At the centre of the cork slab, perspex with dimensions 30 × 4 × 4 cm^3 was inserted. Perspex mimics as lung tumor. A hole was drilled at the centre of perspex for the dose measurements of tumor. Five holes were provided on the cork slab to measure the point dose on central axis and off-axis. Two holes (5 and 10 cm) were made on left and right sides of the centre hole at central axis respectively. The teflon cylindrical rod was placed in the PMMA slab for the dose measurement of spine.

The ionization chamber was placed in the PMMA block to measure the tumor dose. During the exposure of radiation to the particular area, the other holes are completely closed by inserting the respective materials to avoid the air inhomogeneity. Thereafter chamber was removed and inserted into the teflon rod to measure the spine dose. The field size was kept as 15×15 cm^2 and the chamber was irradiated for 200 cGy. Same procedure was followed for the other five holes in the cork to measure the lung dose for the same treatment techniques. Similarly, the same measurement was carried out for the homogeneous phantom. The dimension of the homogeneous phantom reflects the heterogeneous phantom except cork slab. Figure 5 shows the experimental set up of the heterogeneous and homogeneous phantoms.

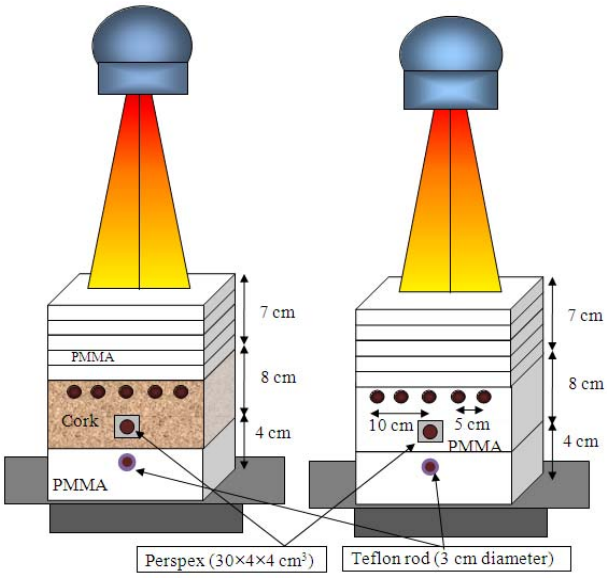

Figure 5. a) Heterogeneous phantom indicating the location of perspex (tumor), cork (lung), Teflon(spine) materials, b) similar homogeneous phantom except cork.

Technique 5

In this technique, thoracic phantom was kept in the top of the couch and the chamber was placed in the perspex chamber's block of tumor. The source to axis distance was set as 80 cm. The field size was kept 15 × 15 cm^2 and the exposure was made about 200 cGy. The dose values were measured for anterior to posterior (AP), right posterior oblique (RPO) and left posterior oblique (LPO) fields (figure 6). The chamber was irradiated for 200 cGy to measure the dose values for "Arc therapy" and "Rotation therapy" with gantry rotations from 345 to 15° (30°), 340 to 25 (45°), 330 to 30° (60°), 325 to 40° (75°), 315 to 45° (90°) and full rotation about 360°. Then, the ionization chamber was placed in perspex, teflon and cork respectively for the both phantoms.

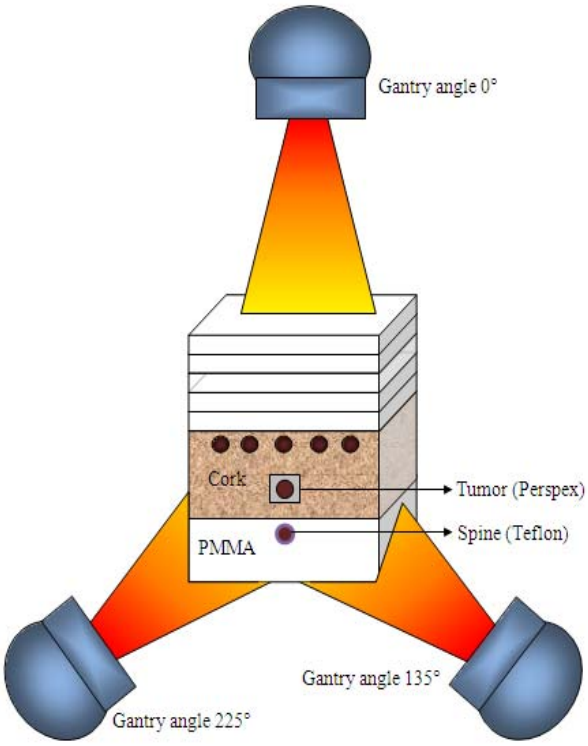

Figure 6. Heterogeneous phantom experimental set up in three field technique for 0˚, 135˚, 225˚esophagus tumor.

Technique 6 (Treatment planning system)

The heterogeneous and homogeneous phantom dose values were compared with 3-D Plato Treatment planning system (TPS). The percentages of deviation were measured for heterogeneous and homogeneous phantoms and compared with TPS. Arc technique for 30, 45, 60, 75, 90 and 360˚ for homogeneous and heterogeneous phantom dose values also compared with TPS. The percentage of deviation was measured.

RESULTS AND DISCUSSION

Ionization chamber was kept at 10 cm depth in the cork and perspex phantoms to determine the inhomogeneity. Field sizes were increased from 5×5 cm^2 to 35×35 cm^2 and meter readings were measured. The measured readings were presented in table 1. Figure 7 shows the meter reading for different field size of cork and PMMA phantoms in SSD and SAD techniques. It is observed from the figure that the meter reading is increased with the field sizes for both phantoms. At fixed field size, the meter reading for the cork phantom is higher than the PMMA phantom. This is due to less attenuation of cork phantom than the PMMA phantom. From the figure, it is also observed that the radiations are attenuated more in PMMA and less in cork. The percentage of deviation for the both phantoms is higher at lower field size and lower at higher field size. The percentage of deviation decreases with the increase in field size up to 22×22 cm^2. There after it remains constant. This implies that the attenuation is same in both the materials at higher field size. The observed reading in SSD technique shows a trend similar to SAD technique. The dose value of SSD technique is higher for the particular field size than the SAD technique where the source to chamber distance is 90 cm. SSD and SAD techniques were used for this measurement and the chamber was kept at 15 cm depth. The measured values for different field sizes were presented in table 2. From the table, it is noted that the meter reading increases linearly with field size for both PMMA and PMMA + cork phantoms. Since the cork is attenuating the radiation less than the PMMA phantom, PMMA + cork phantom values are higher than the PMMA phantom. The percentage of deviation is comparatively less than the 10 cm depth measurement of the phantoms (table 1). Plot of meter reading versus field size of PMMA and PMMA + cork phantoms is shown in figure 8. For the particular field sizes, the deviation observed from this technique is higher than that of SAD technique. Two slabs of cork (each 4 cm) were placed alternatively between the three PMMA slabs (each 4 cm). A cork slab with 4 cm thickness was placed between 12 and 4 cm thickness of PMMA. The ionization chamber was placed at 16.2 cm depth from the top surface of the both phantom respectively.

Table 1. Percentage deviation between cork and PMMA phantoms for SSD and SAD techniques.

Field size (cm^2)	SSD Technique			SAD Technique		
	Meter reading		% Deviation	Meter reading		% Deviation
	Cork	PMMA		Cork	PMMA	
5 × 5	33	29	13.79	41	36	13.89
6 × 6	34	30	13.33	43	37	16.22
8 × 8	36	33	9.09	46	41	12.20
10 × 10	38	35	8.57	49	44	11.36
15 × 15	42	39	7.69	53	49	8.16
20 × 20	44	41	7.32	57	52	9.62
22 × 22	45	42	7.14	58	53	9.43
25 × 25	46	43	6.98	59	54	9.26
30 × 30	46	43	6.98	60	56	7.14
35 × 35	46	43	6.98	60	56	7.14

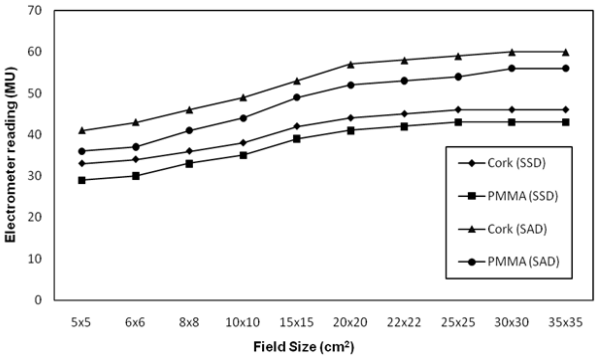

Figure 7. Meter reading Vs field size of cork and PMMA phantoms in SSD and SAD techniques.

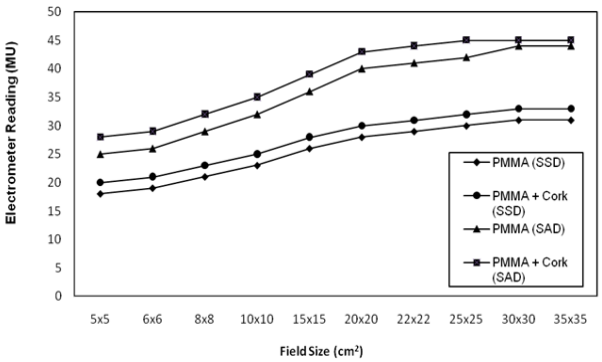

Figure 8. Meter reading Vs field size of PMMA and PMMA + cork phantoms in SSD and SAD techniques.

Table 2. Percentage deviation between PMMA and (PMMA + cork) phantoms for SSD and SAD techniques.

Field size (cm^2)	SSD technique			SAD technique		
	Meter reading		% Deviation	Meter reading		% Deviation
	PMMA	PMMA + cork		PMMA	PMMA + cork	
5 × 5	18	20	10.00	25	28	10.71
6 × 6	19	21	9.52	26	29	10.34
8 × 8	21	23	8.70	29	32	9.38
10 × 10	23	25	8.00	32	35	8.57
15 × 15	26	28	7.14	36	39	7.69
20 × 20	28	30	6.67	40	43	6.98
22 × 22	29	31	6.45	41	44	6.82
25 × 25	30	32	6.25	42	45	6.67
30 × 30	31	33	6.06	44	45	2.22
35 × 35	31	33	6.06	44	45	2.22

The phantoms have been exposed for 200 cGy in SSD and SAD techniques and the measured readings are presented in table 3 and plotted in figure 9. From the figure, the attenuated radiation is found to be low for the higher thickness and high for

the lower thickness of the cork in both techniques of SSD and SAD. The percentage of deviation for the SSD technique is found to be relatively lower than the SAD technique which might be due to the distance between the sources to chamber. The observed percentage of deviation in this technique is less than the previous technique (table 4) which reveals that the higher inhomogeneity reduces the percentage of deviation. Figure 10 shows the dose values at different position in heterogeneous and homogeneous phantoms. The figure depicts that the dose values for both the heterogeneous and homogeneous phantoms are similar to each other and for the particular field the dose value of heterogeneous phantom is higher than the homogeneous phantom. It is also observed that the percentage of deviation is found to be high for the position (1 and 5) lying in the beam edge. The positions (2, 3 and 4) lying in the lung show the low percentage of deviations and having values nearly the same indicating the flatness of the radiation beam. The percentage of deviation of tumor and spine is found to 2.1 and 1.81 respectively which reveals the presence of inhomogeneity. Meter readings of homogeneous and heterogeneous phantoms in tumor and spine were measured for different arc angles such as 30, 45, 60, 75, 90 and 360˚ (table 5). The variation of meter reading with arc angle is shown in figure 11. The dose value of tumor is found to decrease gradually with the increase in arc angle. The dose value of spine is also found to be gradually decreased up to 90˚ and increased in 360˚. For the

Table 3. Percentage deviation between different (PMMA + cork) phantoms for SSD and SAD techniques

Field size (cm^2)	SSD technique		% Deviation	SAD technique		% Deviation
	PMMA + 2 cork	PMMA +1 cork		PMMA +2 cork	PMMA + 1 cork	
5 × 5	18	17	5.55	26	24	8.00
6 × 6	18	17	5.55	27	25	7.70
8 × 8	20	19	5.00	29	27	7.14
10 × 10	22	21	4.54	31	29	6.66
15 × 15	25	24	4.00	36	34	5.71
20 × 20	27	26	3.70	39	37	5.26
22 × 22	28	27	3.57	40	38	5.12
25 × 25	29	28	3.44	42	40	4.87
30 × 30	29	28	3.44	43	41	4.76
35 × 35	29	28	3.44	43	41	4.76

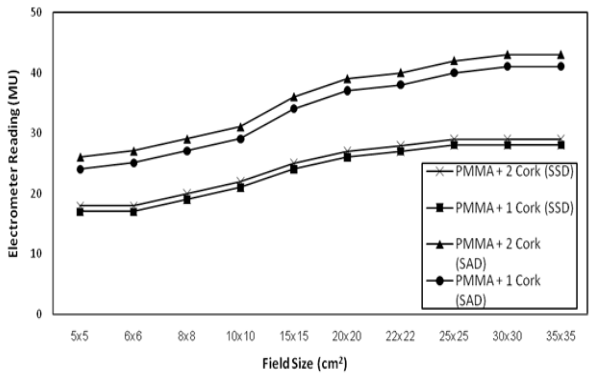

Figure 9. Meter reading Vs field size of different (PMMA + cork) phantoms for SSD and SAD techniques.

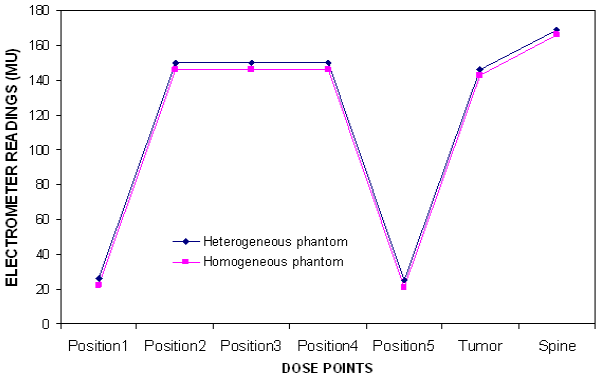

Figure 10. Variation of dose values with different position in the heterogeneous and homogeneous phantoms

particular arc angle, the dose value is higher for heterogeneous tumor and spine than the homogeneous tumor and spine respectively.

The measured dose values for the different positions of homogeneous and heterogeneous phantoms were compared with the TPS values. The values are coinciding with each other and the percentage of deviation varies from 0.47 to 2.8 and 0.49 to 2.86 for heterogeneous and homogeneous phantoms respectively. The data are presented in table 6. The dose values for homogeneous and heterogeneous phantoms of tumor and spine at different arc angles were compared with TPS values and presented in table 7. Ion chamber measured values in the homogeneous and heterogene-

Table 4. Comparison of the monitor units at different positions in the heterogeneous and homogeneous phantoms.

S. No.	Chamber location in phantoms	Heterogeneous phantom (MU)	Homogeneous phantom (MU)	% Deviation
1	Position 1	26	22	18.18
2	Position 2	150	146	2.74
3	Position 3	150	146	2.74
4	Position 4	150	146	2.74
5	Position 5	25	21	19.05
6	Tumor	146	143	2.10
7	Spine	169	166	1.81

Table 5. Comparison of meter reading for the heterogeneous and homogeneous phantoms by arc techniques.

S. No.	Chamber locations in phantom	Meter reading in arc techniques					
		30º	45º	60º	75º	90º	360º
1	Heterogeneous tumor	97	96	94	93	90	76
2	Heterogeneous spine	50	49	48	47	46	59
3	Homogeneous tumor	95	93	92	91	87	72
4	Homogeneous spine	45	44	43	42	40	57

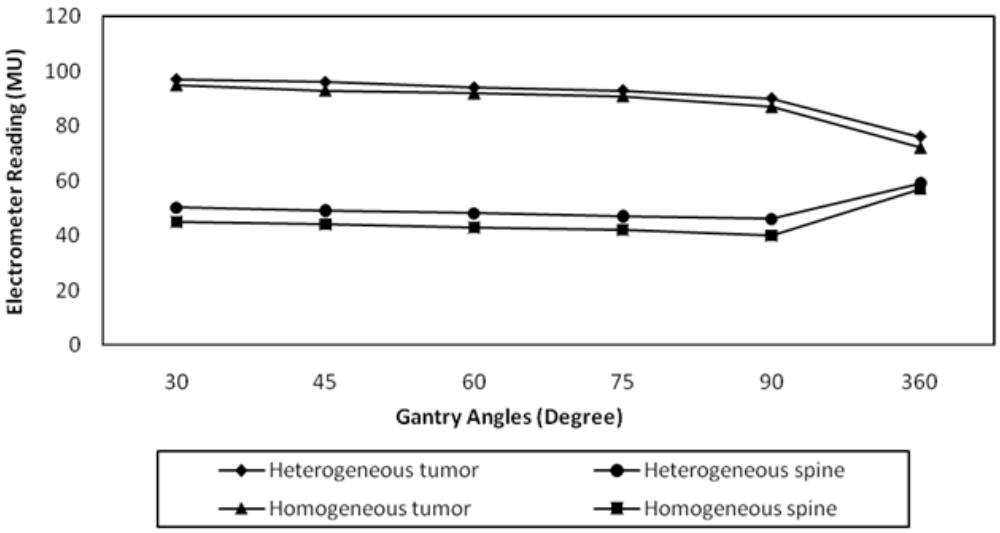

Figure 11. Variation of electrometer reading with different arc angles in the heterogeneous and homogeneous phantoms.

ous phantoms were compared with the TPS values at different angle treatment techniques for tumor and spine. The values coincide with each other and the percentage of deviation is calculated. The percentage of deviation between measured and TPS values of homogeneous and heterogeneous phantoms of tumor vary from 0.32 to 1 and 1.06 to 1.96 respectively. Similarly the percentage of deviation of homogeneous and heterogeneous phantoms of spine varies from 0.99 to 2.3 and 1.25 to 2.79 respectively.

CONCLUSION

Homogeneous and heterogeneous phantoms were successfully fabricated using different tissue equivalent material such us PMMA, cork, teflon and perspex for soft tissue, lung, spine and tumor substitutes respectively. Dosimetric measurements were performed using cobalt-60 gamma rays in tissue equivalent slab homogeneous and heterogeneous phantoms. This phantom was irradiated for different conventional treatment techniques, arc and rotation techniques. The ion chamber measured values and TPS calculated values presented in this study are the characteristic of those obtained for a range of field size, inhomogenity thickness and positions chosen to represent typical geometric encountered in practice. The percentage of deviation for conventional treatment technique was observed for a maximum of 16.22% and minimum of 6.98%. The presence of heterogeneity gives more radiation than

Table 6. Comparison of measured values with TPS values for homogeneous and heterogeneous phantoms.

Chamber location in phantoms	Heterogeneity		% Deviation	Homogeneity		% Deviation
	Measured values	TPS values		Measured values	TPS values	
Position 1	26.0	26.60	2.31	22	22.5	2.27
Position 2	150	150.9	0.60	146	146.8	0.55
Position 3	150	150.7	0.47	146	146.7	0.48
Position 4	150	151.0	0.67	146	147.1	0.75
Position 5	25.0	25.70	2.80	21	21.6	2.86
Tumor	146	147.1	0.75	143	144.6	1.12
Spine	169	170.0	0.59	166	167.4	0.84

Table 7. Comparison of measured values with TPS values for homogeneous and heterogeneous phantoms for different angles.

Arc angle	Tumor in Heterogeneous phantom			Tumor in Homogeneous phantom			Spine in Heterogeneous phantom			Spine in Homogeneous phantom		
	Measured values	TPS values	% Deviation	Measured values	TPS values	% Deviation	Measured values	TPS values	% Deviation	Measured values	TPS values	% Deviation
30º	97	97.5	0.52	50	51	1.60	95	96	1.26	45	46.1	2.44
45º	96	96.7	0.73	49	50	1.84	93	94	1.18	44	45.2	2.73
60º	94	94.6	0.64	48	49	1.46	92	93	1.41	43	44.2	2.79
75º	93	93.3	0.32	47	48	1.06	91	92	0.99	42	43	2.38
90º	90	90.9	1.00	46	47	1.96	87	89	2.30	40	40.5	1.25
360º	76	76.3	0.39	59	60	1.53	72	73	1.81	57	58.4	2.46

homogeneous phantom. The measured values from ion chamber were compared with 3-D Plato Treatment Planning System (TPS). TPS values were also revealed the same result for homogeneous and heterogeneous phantoms. The dose value of tumor is found to be gradually decreased with increase in arc angle. The dose value of spine is also found to be gradually decreased up to 90˚ and increased in 360˚. Significant changes are occurring in and near tissue heterogeneity. These changes are not easily modeled using only physical density. They are dependent upon multiple interconnected factors including density and field size. Dose algorithms that attempt to scale dose only by physical density do not accurately predict dose within or near heterogeneities. During the External Beam Radiation Therapy the presence of heterogeneity will affect the dose distribution. Heterogeneity correction would definitely improve the cancer treatment of the heterogeneity region. This in-house phantom is inexpensive and easy to handle. This is a very reliable tool to measure the dose under heterogeneity condition and it is very useful one to verify the TPS calculation.

REFERENCES

1. Don Robinson (2008) Inhomogeneity correction and the analytic anisotropic algorithm. *J Appl Clini Med Phy,* ***9:*** *112-122.*
2. Felipe Chen Abrego, Carmen Sandra Guzmán Calcina, Adelaide de Almeida, Carlos Eduardo de Almeida, Oswaldo Baffa (2007) Relative output factor and beam profile measurements of small radiation fields with an L-alanine/K-Band EPR minidosimeter. *Med Phys,* ***34:*** *1573-1582.*
3. Yoichi Watanabe, Rob Mooij, Mark Perera G, Marek J. Maryanski (2004) Heterogeneity phantoms for visualization of 3D dose distributions by MRI-based polymer gel dosimetry. *Med Phys,* ***31:*** *975-984.*
4. El-Kathib EE, Battista JJ (1984) Improved lung dose calculation using tissue-maximum ratios in the batho correction. *Med Phys,* ***11:*** *279-286.*
5. El-Kathib EE and Battista JJ (1986) Accuracy of lung dose calculations for large-field irradiation with 6 MV X-rays. *Med Phys,* ***13:*** *111-116.*
6. El-Kathib EE, Evans M, Pla, Cunningham JR (1989) Evaluation of lung dose correction methods for photon irradiations of thorax phantoms. *Int J Radiat Oncol Biol Phys,* ***17:*** *871-878.*
7. Mackie TR, El-Kathib EE, Battista J, Scrimger J, Van Dyk J, Cunningham JR (1985) Lung dose corrections for 6- and 15 MV X- rays. *Med Phys,* ***12:*** *327-332.*
8. Petti PL, Rice RK, Mijnheer BJ, Chin LM, Bjärngard BE (1987) A heterogeneity model for photon beams incorporating electron transport. *Med Phys,* ***14:*** *349-354.*
9. Rice RK, Mijnheer BJ, Chin LM (1988) Benchmark measurements for lung dose corrections for X-ray beams. *Int J Radiat Oncol Biol Phys,* ***15:****399-409.*
10. Engelsman M, Damen EMF, Koken PW, Van't Veld AA, Van Ingen KM, Mijnheer BJ (2001) Impact of simple tissue inhomogeneity correction algorithms on conformal radiotherapy of lung tumours. *Radiother Oncol,* ***60:*** *299-309.*
11. Chetty I J, Charland PM, Tyagi N, McShan DL, Fraas BA (2003) Photon beam relative dose validation of the DPM Monte Carlo code in lung equivalent media. *Med Phys,* ***30:*** *563-573.*
12. Garcia-Vicente F, Minambres A, Jerez I, Modolell I, Perez L, Torres JJ (2003) Experimental validation tests of fast Fourier transform convolutionand multigrid superposition algorithms for dose calculation in low-density media. *Radiother Oncol,* ***67:*** *239-249.*
13. Carrasco P, Jornet N, Duch MA, Panettieri V, Weber L, Eudaldo T, Ginjaume M, Ribas M (2007) Comparison of dose calculation algorithms in slab phantoms with cortical bone equivalent heterogeneities. *Med Phys,* ***34:*** *3323-3333.*
14. Aspradakis MM, Morrison RH, Richmond ND, Steele A (2003) Experimental verification of convolution/ superposition photon dose calculations for radiotherapy treatment planning. *Phys Med Biol,* ***48:*** *2873-2893.*
15. Ekstrand KE, Barnes WH (1990) Pitfalls in the use of high-energy x-rays to treat tumours in the lung. *Int J Radiat Oncol Biol Phys,* ***18:*** *249-252.*
16. Hunt MA, Desobry GE, Fowble B, Coia LR (1997) Effects of low-density lateral interfaces on soft-tissue doses. *Int J Radiat Oncol Biol Phys,* ***37:*** *475-482.*
17. White PJ, Zwicker RD, Huang DT (1996) Comparison of dose homogeneity effects due to electron equilibrium loss in lung for 6 MV and 18 MV photons. *Int J Radiat Oncol Biol Phys,* ***34:*** *1141-1146.*
18. AAPM REPORT NO. 85 tissue inhomogeneity corrections for megavoltage photon beams (2004) Report of Task Group No. 65 of the Radiation Therapy Committee of the American Association of Physicists in Medicine.
19. Rustgi AK, Samuels MA, Rustgi SN (1997) Influence of air inhomogeneities in radiosurgical beams. *Med Dosim,* ***22:*** *95-100.*
20. Solberg TD, Holly FE, DeSalles AAF, Wallace RE, Smathers JB(1995) Implications of tissue heterogeneity for radiosurgery in head and neck tumors. Int J Radiat Oncol Biol Phys, **32:** 235-239.
21. Andrew O. Jones, Indra J. Das, Frederick L. Jones (2003) A monte carlo study of IMRT beamlets in heterogeneous media. *Med Phys,* ***30:*** *296-300.*
22. Papanikolaou N, Battista JJ, Boyer AL, Kappas C, Klein EE, Mackie TR, Sharpe M, Van Dyk J (2004) Tissue inhomogeneity corrections for megavoltage photon beams. AAPM Task Group No. 65 Radiation Therapy Committee.
23. Carrasco P, Jornet N, Duch MA, Weber L, Ginjaume M, Eudaldo T, Jurado D, Ruiz A, Ribas M (2004)Comparison of dose calculation algorithms in phantoms with lung

equivalent heterogeneities under conditions of lateral electronic disequilibrium. *Med Phys,* ***31:*** *2899-2911.*

24. Jones AO and Das IJ (2005) Comparison of inhomogeneity correction algorithms in small photon fields. *Med Phys,* ***32:*** *766-776.*
25. Jeraj R, Keall PJ, Siebers JV (2002) The effect of dose calculation accuracy on inverse treatment planning. *Phys Med Biol,* ***47:*** *391-407.*
26. Ma C, Pawlicki T, Jiang SB, Li J, Deng J, Mok E, Kapur A, Xing L, Ma L, Boyer AL (2000) Monte Carlo verification of IMRT dose distributions from a commercial treatment planning optimization system. *Phys Med Biol,* ***45:*** *2483-2495.*
27. Vanderstraeten B, Reynaert N, Paelinck L, Madani I, Wagter CD, Gersem WD, Neve WD, Thierens H (2006) Accuracy of patient dose calculation for lung IMRT: A comparison of Monte Carlo, convolution/ superposition, and pencil beam computations. *Med Phys,* ***33:*** *3149-3158.*
28. Butson MJ, Elferink R, Cheung T, Yu K, Stokes M, Quach Y, Metcalfe P (2000) Verification of lung dose in an anthropomorphic phantom calculated by the collapsed cone convolution method. *Phys Med Biol,* ***45:*** *143-149.*
29. McDermott PN and He T, DeYoung A (2003) Dose calculation accuracy of lung planning with a commercial IMRT treatment planning system. *J Appl Clin Med Phys,* ***4:*** *341-351.*
30. Scott E. Davidson, Geoffrey S. Ibbott, Karl L. Prado, Lei Dong, Zhongxing Liao, David S (2007) Accuracy of two heterogeneity dose calculation algorithms for IMRT in treatment plans designed using an anthropomorphic thorax phantom. *Med Phys,* ***34:****1850-1857.*
31. Low DA and Mutic S (1997) Abutment region dosimetry for sequential arc IMRT delivery. *Phys Med Biol,* ***42:*** *1465-1470.*
32. Stein J, Mohan R, Wang XH, Bortfeld T, Wu Q, Preiser K, Ling CC, Schlegel W (1997) Number and orientations of beams in intensitymodulated radiation treatments. *Med Phys,* ***24:*** *149-160.*
33. Serago CF, V. Houdek P, Hartmann GH, Saini DS, Serago ME, Kaydee A (1992) Tissue maximum ratios (and other parameters) of small circular 4, 6, 10, 15 and 24 MV x-ray beams for radiosurgery. *Phys Med Biol,* ***37:*** *1943-1956.*
34. Rustgi SN and Frye DMD (1995) Dosimetric characterization of radiosurgical beams with a diamond detector. *Med Phys,* ***2:*** *2117-2121.*